

The Renaissance and Promise of Electron Energy-Loss Spectroscopy**

Sir John Meurig Thomas*

atomic resolution · electronic structure ·
time-resolved spectroscopy · graphite · plasmons

*Dedicated to Professor Joachim Sauer
on the occasion of his 60th birthday*

It has long been known^[1] that by measuring the discrete “loss” peaks suffered by primary beams of monoenergetic electrons after they have penetrated thin films of metals, it is possible quantitatively to determine the trace amounts of carbon, nitrogen, or oxygen present in those metals. Thus, electron energy-loss (EEL) peaks at approximately 285, 400, or 530 eV signify the presence of carbon, nitrogen, or oxygen, these being respectively their K-shell ionization energies. In the early 1970s, commercial electron microscopes began to be equipped with (postspecimen) electron spectrometers, and soon EEL spectroscopy gained prominence as a useful characterizing tool.^[2] Under ideal conditions not only was it possible to discover the composition and thickness (from the position and attenuated signals of the loss peaks) of the investigated specimens, but also, as outlined elsewhere,^[2–4] the atomic environment (coordination sphere), bond distances, and oxidation state of the element responsible for the EEL could be derived from the fine structure (near-edge and extended-edge) of the loss peak.

Subsequent developments enabled EELS spectra to be recorded more readily and precisely, but the transformative advances in technique that have occurred very recently have led to a renaissance in this method of characterizing solids. Owing to vast improvements in detectors, it is now possible to reveal the presence—and to determine the oxidation state—of a few ions, weighing a mere zeptogram (10^{-21} g) or so. For example, Suenaga, Sato, and co-workers^[5] identified the precise location of individual Ce^{3+} and Ce^{4+} ions incarcerated inside fullerenes and carbon nanotubes. Moreover, using an aberration-corrected scanning transmission electron microscope (STEM) that provides a 100-fold increase in signal, Muller et al.^[6] were able to construct a full two-dimensional chemical map of multilayer perovskitic solids by EELS, which also contained both bonding and electronic information.

It is not only inorganic materials that may be characterized by EELS, with all its built-in advantages of high spatial discrimination that is particularly well suited for probing heterogeneous (compositionally variable) materials; biological specimens, especially cellular ones, are also amenable to elucidation by this technique. Thus, Leapman et al.^[7] have shown that: 1) the total distribution of biomolecules, including proteins and nucleic acids, emerges from the intensity of the K-shell (nitrogen) EELS signal; 2) the proteins that contain high levels of the amino acids cysteine and methionine can be deduced from the sulfur EELS signal; and 3) the distribution of nucleic acids, phosphorylated proteins, and phospholipids follows from phosphorous EELS signals.

EELS spectra and the closely related procedure of energy-filtered transmission electron microscopy (EFTEM) yield a wealth of compositional and structural information; and by combining electron tomography^[8] and EELS, such that at every tilt angle required to accumulate the tomogram the energy-filtered image is also recorded, it is possible to determine noninvasively and nondestructively the composition of a minute volume in the interior of a specimen down to the sub-attogram (10^{-18} g) level. This method was first used by Midgley et al.^[9] in their nanochemical characterization of nylon-multiple-wall carbon nanostructures.

Impressive as the contribution of static EEL spectroscopy has been to solid-state and surface chemistry,^[3] much more can be gained by introducing the time dimension to its measurement. Static, time-integrated EEL spectra do not provide direct dynamic information, and, to date, video-rate scanning in an electron microscope has achieved a time resolution of only a few milliseconds or so. To achieve a picture of the dynamics of chemical bonding from the valence electrons in solids that provide insights into electronic structure, the time resolution must be increased by at least nine orders of magnitude. In this way it should be possible, by recording loss spectra in the energy range 0 to 50 eV, to retrieve information which, hitherto, was thought to be achievable only by synchrotron-based X-ray absorption spectroscopy.^[10,11] Two recent papers^[12,13] from the Zewail group, using their ultrafast electron microscope (UEM),^[14,15] demonstrate that this goal can be reached, thus allowing chemical bonding to be monitored directly by energy-resolved 4D electron microscopy.

The solid they selected for a case study of the valence electrons was graphite, an archetypal semimetal that has

[*] Prof. Sir J. M. Thomas
Department of Materials Science and Metallurgy
University of Cambridge
Pembroke Street, CB2 3QZ, Cambridge (UK)
Fax: (+44) 1223-334-300
E-mail: jmt2@cam.ac.uk

[**] I am grateful to A. H. Zewail, J. C. H. Spence, and C. Ducati for stimulating conversations and to this Department for financial support.

delocalized π orbitals and bonding within the planes where the orbitals on carbon are sp^2 hybrids. The static EEL spectrum of graphite is shown in Figure 1, where the various plasmon characteristics are labeled. (Plasmons are quanta of plasma oscillations.) In graphite there are π plasmons as well as $\pi + \sigma$ plasmons; and there are surface plasmons in addition to bulk ones, with well-known^[16] values that are shown in Figure 1.

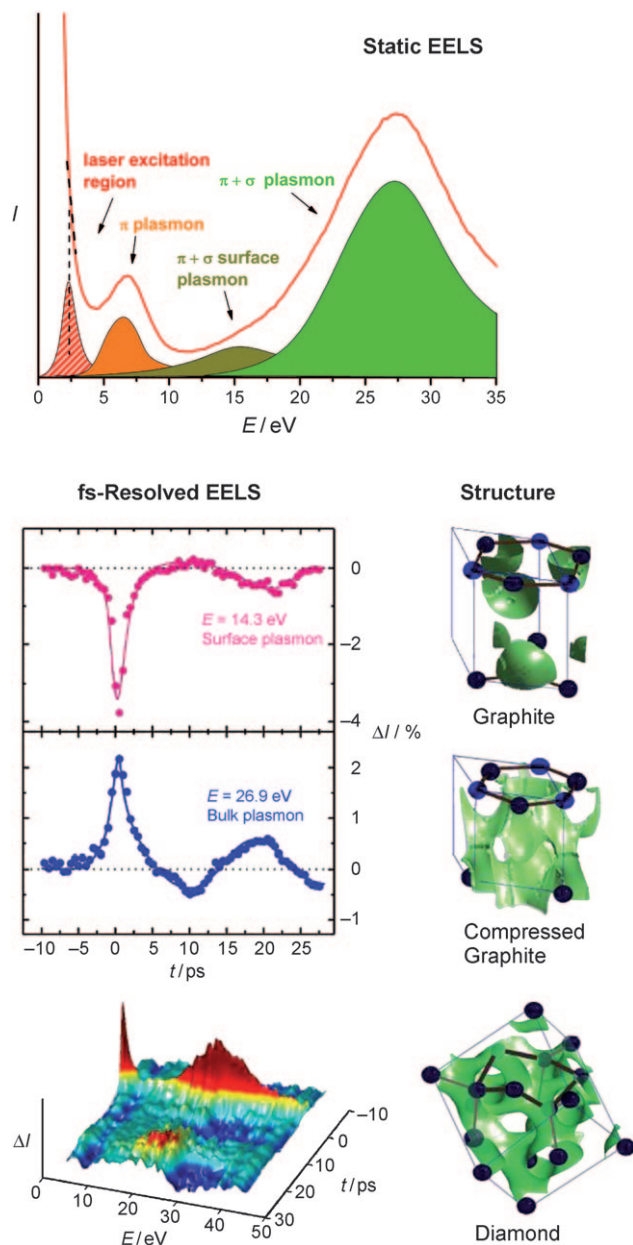


Figure 1. Top: The static EEL spectrum of graphite. The red line denotes the loss spectrum at negative time. The π plasmon occurs around 7 eV, whilst the $\pi + \sigma$ plasmon for the bulk graphite is around 27 eV, and the surface $\pi + \sigma$ plasmon is around 15 eV. Also shown at 2.4 eV is the energy of the photogenerated electron-hole (carrier) plasma that is absent from the static EEL spectrum.^[12] Bottom: Femtosecond-resolved EELS of graphite (left). Shown on the right is the electron density distribution (green) in graphite and the manner in which it changes on the femtosecond timescale (upon compression by a laser pulse) into diamond.^[13]

What, in effect, Zewail and co-workers have done is to map the dynamics of the electronic state of the valence electrons in graphite at the femtosecond level.^[17] By delivering a 2.4 eV (laser light) pulse on to the specimen over a duration of 220 fs, and recording directly the EEL spectrum at a repetition rate sufficient to allow the specimen to cool (starting from negative time up to 5 ps) in their electron microscope, they recorded time frames and the difference between the graphite EEL spectrum at a given time and that at zero time, thereby directly following the fate of the plasmons after the arrival of the excitation initial pulse. Upon impact of the laser pulse on the specimen the graphite is seen^[12,13] to undergo a compression of the layers, followed some 2 ps later by their gradual expansion.

Interestingly, whereas the 7 eV π plasmon peak remains nearly unperturbed by the excitation, there is an increase in the intensity of the bulk $\pi + \sigma$ plasmon upon compression. But as the individual layers are separated and reach the graphene (isolated-layer) limit, it transpires, as expected on theoretical grounds, that only the surface $\pi + \sigma$ plasmon, at a value of approximately 15 eV, survives.

Carbone et al.^[13] show that the degree of non-equilibrium compression and subsequent expansion of the graphene layers in graphite (which is governed by the fluence of the excitation pulse) is correlated with the direction of change from sp^2 to sp^3 (i.e. 3D-diamond-like structure) electronic hybridization, and these authors find that their results are in line with those derived from theoretical charge-density calculations. Their work now opens the door to experiments that can follow the ultrafast dynamics of the electronic structure of solids in general. With the reality of achieving even shorter optical pulses,^[18] the Zewail group has provided the methodology^[19] to generate attosecond (10^{-18} s) electron pulses for imaging and for EELS—on the timescale at which electrons move. With the achievement of femtosecond-resolved EELS and the extension to the attosecond domain, there is the promising prospect that a table-top UEM–EELS facility may well provide real-time structural and electronic information hitherto thought possible only using certain types of synchrotrons and free-electron lasers.^[20]

Received: July 22, 2009

Published online: October 14, 2009

- [1] a) E. Rudberg, *Proc. R. Soc. London Ser. A* **1930**, 127, 111; b) G. Ruthemann, *Naturwissenschaften* **1941**, 29, 648.
- [2] a) J. M. Thomas in *Inorganic Chemistry: Towards the 21st Century* (Ed.: M. H. Chisholm), American Chemical Society, Washington, **1983**, pp. 445–472 (ACS Symposium Series 211); b) R. F. Egerton in *Electron Energy-Loss Spectroscopy in the Electron Microscope*, 2nd ed., Plenum, New York, **1996**; c) R. F. Egerton, *Top. Catal.* **2002**, 21, 185.
- [3] J. M. Thomas, B. G. Williams, T. G. Sparrow, *Acc. Chem. Res.* **1985**, 18, 324.
- [4] J. H. C. Spence, *Rep. Prog. Phys.* **2006**, 69, 725. See especially the section on complications arising from multiple scattering, and channeling.
- [5] K. Suenaga, Y. Sato, Z. Liu, H. Kataura, T. Okazaki, K. Kimoto, H. Sawada, T. Sasaki, K. Omoto, T. Tomita, T. Kaneyama, Y. Kondo, *Nat. Chem.* **2009**, 1, 415.

- [6] D. A. Muller, L. Fitting Kourkoutis, M. Murfitt, J. H. Song, H. Y. Hwang, J. Silcox, N. Dellby, O. L. Kriwanek, *Science* **2008**, 319, 1073.
- [7] a) R. D. Leapman, C. E. Fioni, K. E. Gorlen, C. C. Gibson, C. R. Swift, *Ultramicroscopy* **2004**, 100, 115; b) M. A. Aronova, Y. C. Kim, R. Harman, A. A. Sousa, G. Zhang, R. D. Leapman, *J. Struct. Biol.* **2007**, 160, 35.
- [8] P. A. Midgley, E. W. Ward, A. B. Hungria, J. M. Thomas, *Chem. Soc. Rev.* **2007**, 36, 1477.
- [9] M. H. Grass, K. K. Koziol, A. H. Windle, P. A. Midgley, *Nano Lett.* **2006**, 6, 376.
- [10] J. C. H. Spence, M. R. Howells, *Ultramicroscopy* **2002**, 93, 213.
- [11] A. P. Hitchcock, J. J. Dynes, G. Johansson, J. Wang, G. Botton, *Micron* **2008**, 39, 311.
- [12] F. Carbone, B. Barwick, O-H Kwon, H. S. Park, J. Spencer Baskin, A. H. Zewail, *Chem. Phys. Lett.* **2009**, 468, 107.
- [13] F. Carbone, O-H Kwon, A. H. Zewail, *Science* **2009**, 325, 181.
- [14] A. H. Zewail, *Annu. Rev. Phys. Chem.* **2006**, 57, 65.
- [15] B. Barwick, H. S. Park, O. H. Kwon, J. S. Baskin, A. H. Zewail, *Science* **2008**, 322, 1227.
- [16] E. A. Taft, H. R. Philipp, *Phys. Rev.* **1965**, 138, A197.
- [17] The fs-resolved EELS data were recorded in Zewail's ultrafast electron microscope operating in the single-electron per pulse mode. A train of 220 fs infrared laser pulses ($\lambda = 1038$ nm) was split into two paths; one was frequency-doubled and used to excite the specimen of the graphite on the microscope grid, and the other was frequency-tripled into the UV and directed to the photoemissive cathode to generate the electron packets. These pulses were accelerated in the electron microscope column and dispersed after transmission through the sample to provide the EEL spectrum. Details of the clocking are given in references [12] and [13].
- [18] a) P. B. Corkum, F. Krausz, *Nat Phys.* **2007**, 3, 381; b) F. Krausz, M. Ivanov, *Rev. Mod. Phys.* **2009**, 81, 163.
- [19] a) P. Baum, A. H. Zewail, *Proc. Nat. Acad. Sci. USA* **2007**, 104, 18409; b) S. A. Hibbert, C. Uiterwaal, B. Barwick, H. Batelaan, A. H. Zewail, *Proc. Natl. Acad. Sci. USA* **2009**, 106, 10558; c) A. H. Zewail, J. M. Thomas, *4D Electron Microscopy*, Imperial College Press, London, **2009**.
- [20] H. N. Chapman, *Nat. Mater.* **2009**, 8, 299 (Insight-Commentary).